Molecular Cancer Therapeutics

Molecular Basis of Valine-Citrulline-PABC Linker Instability in Site-Specific ADCs and Its Mitigation by Linker Design

Magdalena Dorywalska[1], Russell Dushin[2], Ludivine Moine[2], Santiago E. Farias[1], Dahui Zhou[2], Thayalan Navaratnam[2], Victor Lui[1], Adela Hasa-Moreno[1], Meritxell Galindo Casas[1], Thomas-Toan Tran[1], Kathy Delaria[1], Shu-Hui Liu[1], Davide Foletti[1], Christopher J. O'Donnell[2], Jaume Pons[1], David L. Shelton[1], Arvind Rajpal[1], and Pavel Strop[1]

Abstract

The degree of stability of antibody–drug linkers in systemic circulation, and the rate of their intracellular processing within target cancer cells are among the key factors determining the efficacy of antibody–drug conjugates (ADC) *in vivo*. Previous studies demonstrated the susceptibility of cleavable linkers, as well as auristatin-based payloads, to enzymatic cleavage in rodent plasma. Here, we identify Carboxylesterase 1C as the enzyme responsible for the extracellular hydrolysis of valine-citrulline-*p*-aminocarbamate (VC-PABC)-based linkers in mouse plasma. We further show that the activity of Carboxylesterase 1C towards VC-PABC–based linkers, and consequently the stability of ADCs in mouse plasma, can be effectively modulated by small chemical modifications to the linker. While the introduced modifications can protect the VC-PABC–based linkers from extracellular cleavage, they do not significantly alter the intracellular linker processing by the lysosomal protease Cathepsin B. The distinct substrate preference of the serum Carboxylesterase 1C offers the opportunity to modulate the extracellular stability of cleavable ADCs without diminishing the intracellular payload release required for ADC efficacy. *Mol Cancer Ther; 15(5); 958–70. ©2016 AACR.*

Downloaded from http://aacrjournals.org/mct/article-pdf/15/5/958/1851970/958.pdf by guest on 24 August 2022

Introduction

Antibody–drug conjugates (ADC) are a growing class of cancer therapeutics with promising clinical outcomes. Most ADCs exert their activity by a mechanism that involves an antibody-directed delivery of potent cytotoxic drugs specifically to the target-expressing cells where they are released only after target-mediated internalization. This approach can maximize therapeutic potential and minimize unwanted side effects, offering an advantage over conventional chemotherapy (1, 2). The attachment of the cytotoxic drug to the antibody relies on one of two general types of chemical linkers, cleavable or noncleavable, both of which require intracellular processing to allow for release of the active cytotoxic species (3). Premature loss of the payload prior to ADC internalization into the target cell can have a number of undesirable consequences including reduced potency, possible competition of naked antibody against the intact ADC for target binding, as well as off-target toxicity from nontarget–specific drug release (4–6).

Diverse examples of conjugates with cleavable or noncleavable linkers are currently in development. Various degrees of instability in the systemic circulation have been observed for many ADCs bearing commonly utilized linkers, such as the decoupling of the maleimide-based linker payloads resulting in reduced ADC exposure, the premature loss of disulfide-linked payloads leading to shortened pharmacokinetic profiles, as well as the degradation of the payload moiety itself (7–9).

The widely used valine-citrulline-*p*-aminocarbamate (VC-PABC) dipeptide linker has been popularized as a way to maintain a stable covalent attachment of the drug to the antibody that could be preferentially cleaved by intracellular protease(s) of the lysosomal degradation pathway (10–12). The VC-PABC–based linkers display a superior systemic stability over other cleavable linkers, and constitute the most commonly applied cleavable linkage technology among ADCs currently in clinical development. However, we observed that site-specific conjugates carrying the cleavable aminocaproyl-VC-PABC-Aur0101 (C6-VC-PABC-Aur0101) linker-payload can be hydrolyzed in mouse and rat plasma prior to their internalization (13, 14). The process appears to be enzyme mediated, is largely dependent on the conjugation site, and reduces ADC potency both *in vitro* and *in vivo* (14).

Interestingly, when we examined the stability of noncleavable site-specific conjugates in rodent plasma, we observed an enzymatic degradation of the C-terminal portion of the amino-PEG6-propionyl-MMAD (PEG6-C2-MMAD) linker-payload, showing a similar dependence on conjugation position (9). While it was unclear whether the C6-VC-PABC linker cleavage and the degradation of MMAD payload might be due to the activity of the same

[1]Rinat Laboratories, Pfizer Inc., South San Francisco, California. [2]Worldwide Medicinal Chemistry, Pfizer Inc., Groton, Connecticut.

Note: Supplementary data for this article are available at Molecular Cancer Therapeutics Online (http://mct.aacrjournals.org/).

Current address for T. Navaratnam: Toronto Research Chemicals, 2 Brisbane Road, Toronto, Ontario M3J 2J8, Canada; current address for D. Foletti: 23andMe, 899 W Evelyn Ave, Mountain View, CA; current address for J. Pons: Alexo Therapeutics, 951 Gateway Blvd Ste 201, South San Francisco, CA 94080; and current address for A. Rajpal: Bristol-Myers Squibb, 700 Bay Rd Ste A, Redwood City, CA 94063.

Corresponding Author: Pavel Strop, Bristol-Myers Squibb, 700 Bay Rd Ste A, Redwood City, CA 94063. Phone: 650-260-9968; E-mail: pavel.strop@bms.com

doi: 10.1158/1535-7163.MCT-15-1004

©2016 American Association for Cancer Research.

or different enzyme(s), both processes were sensitive to the same protease inhibitors that suggested a serine-dependent hydrolase mechanism (9, 14).

Although cynomolgus monkey and human species appear to have negligible levels of both cleavable and noncleavable linker-payload degradation in plasma stability assays, either type of conjugate must undergo rodent studies where the described linker-payload instability can have significant effects on efficacy. This differential ADC stability between rodent and primate species can lead to difficulties in evaluating the efficacy of a drug candidate, largely performed in mouse models, relative to its safety, typically tested in non-human primate models.

Here, we identify the serine hydrolase responsible for the extracellular cleavage of VC-PABC-containing linker-payloads in mouse plasma as Carboxylesterase 1C (Ces1C). We show that mouse Ces1C in its purified form, as well as in the context of mouse plasma, is sensitive to chemical derivatization of the linker which can modulate its VC-PABC hydrolysis activity. We further demonstrate that modifications of the VC-PABC linkers that are resistant to mouse Ces1C cleavage do not have the same effect on the human Cathepsin B (CatB), the lysosomal protease responsible for intracellular linker processing and release of the drug moiety. This distinct linker substrate preference of the two enzymes offers the ability to modulate the extracellular stability of the VC-PABC–linked conjugates in rodent circulation without interfering with the intracellular linker processing in the lysosomal degradation pathway of the target cell. Comparison between the structures of the human liver carboxylesterase homolog and human lysosomal CatB offers a possible explanation for the differential substrate selectivity of the two enzymes.

Materials and Methods

Protein purification, conjugation, and analytics

For site-specific conjugation using microbial transglutaminase, several glutamine-containing sites were engineered into the anti-M1S1 C16 antibody as described previously (13, 14), and they were as follows: site A, light chain residues 200-202 replaced by LLQG tag; site B, insertion of LLQG tag at position 160 in the heavy chain; site C, insertion of LLQG tag at position 135 in the heavy chain; site D, replacement of residue 447 with LLQGA tag in the heavy chain; site E, heavy chain residues 190-192 replaced by LLQG tag; site F, insertion of GGLLQGPP tag after residue 214 in the light chain; site G, N297A deglycosylation mutant where conjugation happens at native Q295 on the heavy chain; site H, N297Q mutant where conjugation happens on Q295 and Q297 on the heavy chain (15); site I, heavy chain residues 294-297 replaced with LLQG tag. Protein purification and conjugation were carried out as reported previously (13, 14). Drug–antibody loading was assessed using hydrophobic interaction chromatography (HIC) or liquid chromatography/mass spectrometry (LC/MS) intact mass analysis as described previously (13, 14, 16).

For preparation of the conventional C16-maleimido-caproyl-VC-PABC-Aur0101 conjugate with an average drug–antibody ratio (DAR) of 4, 4.4 mg/mL antibody was reduced using 216 μmol/L TCEP in 25 mmol/L Tris HCl pH 7.5, 150 mmol/L NaCl for 2 hours at 37°C, followed by addition of 283 μmol/L linker-payload and incubation for 1 hour at room temperature. Conjugate was then dialyzed against PBS to remove excess unreacted linker-payload.

In vitro stability and inhibitor assays

Serum and plasma from different species were obtained from BioreclamationIVT. Conjugates were tested for stability *in vitro* in whole plasma, whole serum, or fractionated serum following described protocols (9, 14). Typically, 0.125 mg/mL ADC was incubated in 62.5% (v/v) plasma diluted in 1× PBS. Inhibitors (Roche, Sigma) were added to reactions as indicated prior to the addition of substrates.

Fractionation of mouse serum for enrichment of linker hydrolase activity

To identify the enzyme responsible for VC-PABC linker cleavage in mouse plasma, we enriched the linker hydrolysis activity by fractionating the Balb/c mouse serum using a sequence of steps. First, Balb/c serum (BioreclamationIVT) was depleted of IgG and albumin using commercially available MabSelect Protein A and Protein G resins (GE Healthcare), followed by Qproteome Murine Albumin Depletion Kit (Qiagen). The depleted serum was then subjected to sequential precipitation with ammonium sulfate. Linker hydrolase activity was determined for each fraction by incubating with the C16 Site A-C6-VC-PABC-Aur0101 substrate at 37°C for 18 to 20 hours, followed by protein precipitation with 5 volumes of acetonitrile, and using an liquid chromatography/tandem mass spectrometry (LC/MS-MS) method to assess the amount of free 0101 payload present in the soluble portion. Fractions with the highest linker hydrolase activity were then applied to cation exchange HiTrap SP column (GE Healthcare) equilibrated with 100 mmol/L sodium acetate buffer pH 5.2, and eluted using step gradient elutions with sodium chloride. SP fractions with the highest activity were applied to anion exchange HiTrap Q column (GE Healthcare) equilibrated with 100 mmol/L Tris hydrochloride buffer pH 8.5, and eluted using step gradient elutions with sodium chloride. Fractions with the highest hydrolase activity were then combined and size fractionated using Superdex 200 column (GE Healthcare), following by the final depletion of the high abundance serum proteins using the Top 3 column (Agilent). The final enriched fraction was subjected to activity and inhibition assays, as well as proteomic analysis.

LC/MS-MS analysis of the free 0101 payload released in hydrolase activity assays

Serum fractions were tested for hydrolase activity in the presence of C16 Site A-C6-VC-PABC-Aur0101, followed by precipitation with 5 volumes of acetonitrile, and removal of insoluble material by centrifugation. A 5 μL aliquot of each sample was injected onto an HPLC system, using hydrophilic interaction chromatography (HILIC) column separation (Waters, XBridge BEH HILIC XP Column, 2.1 mm, 50 mm, 2.5 μm). Samples were eluted at a flow rate of 400 μL/minute with a linear gradient using water as mobile phase A, and acetonitrile as mobile phase B, both in 0.1% formic acid. The gradient elution used was as follows: 0–1 minute 97% B; 1–4 minutes 3–55% B; 4–4.1 minutes 55–2% B; 4.1–5 minutes 2% B; 5–5.1 minutes 2–97% B; and 5.1–15 minutes 97% B. The HPLC effluent was directly connected to the electrospray source of a triple quadrupole mass spectrometer (Applied Biosystems API 4000). The 0101 payload was detected in positive ion mode using multiple reaction monitoring of the specific transitions: m/z 743 → 188, 743 → 374, and 743 → 559. The relative abundance of 0101 was measured as the area under the curve for transition m/z 743 → 188.

Downloaded from http://aacrjournals.org/mct/article-pdf/15/5/958/1851970/958.pdf by guest on 24 August 2022

Proteomic analysis of serum fraction enriched for hydrolase activity

Samples (10–50 μg) were solubilized in 0.2% RapiGest (Waters Corp, 186001861) and 20 mmol/L ammonium bicarbonate. The samples were then incubated at 80°C for 15 minutes. Dithiothreitol (DTT, 3 mmol/L final concentration) was added to the samples, and incubated at 60°C for 30 minutes to reduce disulfide bonds. After the samples were cooled to room temperature, iodoacetamide (IAA, 9 mmol/L final concentration) was added, and then samples were incubated at room temperature for 30 minutes in the dark to alkylate-reduced cysteines. Modified trypsin (Promega, cat #V5111 or cat #V1651) was added (1:100 enzyme/substrate) and the samples were incubated at 37°C overnight. To hydrolyze the RapiGest prior to mass spectrometry analysis, TFA was added to a final concentration of 0.5%. The solution was incubated at 37°C for 90 minutes, and then centrifuged at 20,800 × *g* at 4°C for 30 minutes. Samples (1 μg of digested protein) were loaded into a nano C18 column (Precision capillary columns, 100 μm × 150 mm, 3 μm), and eluted at 35°C with a flow rate of 0.3 μL/minute. LC/MS-MS analysis was performed using nano LC system (Dionex, Ultimate 3000), coupled to an Orbitrap Velos Pro (Thermo Scientific) mass spectrometer with Nanospray Flex ion source. Peptides were separated by gradient elution using water as mobile phase A, and 80% acetonitrile as mobile phase B, both in 0.1% formic acid. The gradient elution used was as follows: 0–40 minutes 3% B; 40–100 minutes 3–50% B; 100–100.1 minutes 50–95% B; 100.1–102 minutes 95% B; 102–102.1 minutes 95–3% B; and 102.1–120 minutes 3% B. The Orbitrap Velos was operated in information dependent acquisition (IDA) mode with CID performed on the top 10 ions. The MS scan was performed in the Orbitrap at 100,000 resolution, whereas the fragment spectra were collected in the low pressure trap. Ion trap and Orbitrap maximal injection times were set to 50 and 500 ms, respectively. The ion target values were 30,000 for the ion trap, and 1,000,000 for the Orbitrap. The raw data file was converted to mgf file, and searched against Swiss-Prot reviewed database using Mascot software. Finally, the data were visualized and validated using Scaffold software.

LC/MS intact mass analysis

ADCs were deglycosylated with PNGase F (NEB, cat #P0704L) under nondenaturing conditions at 37°C overnight. For light chain and heavy chain analysis, deglycosylated samples were reduced with 20 mmol/L (DTT) for 30 minutes at 60°C. ADCs (500 ng) were loaded into a reverse-phase column packed with a polymeric material (Michrom-Bruker, cat #CM8/00920/00). LC/MS analysis was performed using Agilent 1100 series HPLC system, comprising binary HPLC pump, degasser, thermostatted auto sampler, column heater, and diode-array detector (DAD), coupled to an Orbitrap Velos Pro (Thermo Scientific) mass spectrometer with electrospray ion source. The resulting mass spectra were deconvoluted using ProMass software (Thermo Fisher Scientific).

Cloning and expression of recombinant mouse Ces1C

A construct encoding amino acids 19-547 of mouse Ces1C with the mouse IgG heavy chain signal peptide MEWSWVFLFFLSVTTGVHS at the N-terminus, and a C-terminal HIS tag was expressed in Expi293 mammalian cells. The secreted protein was purified from the filtered culture media using affinity chromatography with Ni-NTA resin (Qiagen) following manufacturer's protocols.

Western blot analysis

Purified recombinant mouse Ces1C (10–100 ng), and whole mouse serum (0.5 μL) were resolved by SDS-PAGE, and transferred to a nitrocellulose membrane using iBlot Gel Transfer Device (Thermo Fisher Scientific). The membrane was blocked with 3% BSA, and blotted with the rabbit anti-mouse Ces1C polyclonal antibody (Abcam), followed by the IRDye 800CW goat anti-rabbit antibody (LI-COR Biosciences) to allow visualization of bands using the Odyssey Infrared Imaging System (LI COR Biosciences).

Enzymatic activity assays

Recombinant mouse Ces1C was purchased from MyBioSource. Recombinant mouse Ces1G, recombinant mouse CatB, and recombinant human Ces1 were purchased from R&D Systems. Human CatB purified from liver, and recombinant human Ces2 were purchased from Sigma. Human CatB and mouse CatB were activated in the presence of 1.2 mmol/L L-cysteine and 0.75 mmol/L EDTA at 40°C for 10 minutes, and 0.5 μg/mL enzyme was reacted with 0.125 mg/mL ADC in 120 mmol/L potassium phosphate pH 6.0. For mouse Ces1C, mouse Ces1G, human Ces1, and human Ces2, 0.5–240 μg/mL enzyme was incubated with 0.125 mg/mL ADC in PBS. Inhibitors (Roche, Sigma) were added to reactions prior to the addition of substrates as needed. Enzymatic reactions were carried out at 37°C for 2 to 120 hours as indicated. Conjugates were isolated using MabSelect SuRe beads or M1S1 antigen coupled to CNBr-activated Sepharose (GE Healthcare, Inc.). DAR values were assessed using HIC or mass spectrometry methods.

Knockout mice

Heterozygous *Ces1C*$^{+/-}$ mice (strain B6(Cg)-*Ces1c*$^{tm1.1Loc}$/J) were obtained from The Jackson Laboratories. Offspring obtained from *Ces1C*$^{+/-}$ *mice* were genotyped to identify the *Ces1C*$^{+/+}$, *Ces1C*$^{+/-}$, and *Ces1C*$^{-/-}$ individuals.

Pharmacokinetic studies

All animal experiments were conducted in an Association for Assessment and Accreditation of Laboratory Animal Care accredited facility under Institutional Animal Care and Use Committee–approved protocols. For pharmacokinetic experiments to monitor stability of different linkers, C16 Site F conjugates featuring modified VC-PABC-Aur0101 linker-payloads were administered into female CB17 SCID mice ($n = 3$) in a single 9 mg/kg dose. Serum samples were collected at appropriate time points for 3 or 10 days as indicated. Total antibody and ADC ELISA assays were carried out as described previously (14).

For pharmacokinetic experiments in *Ces1C*$^{+/+}$ and *Ces1C*$^{-/-}$ mice, a single intravenous dose of 6 mg/kg of C16 Site F-Linker 1-VC-PABC-Aur0101 conjugate was administered into male and female mice ($n = 4$). Serum samples were withdrawn at appropriate time points over 10 days as indicated. Total antibody and ADC ELISA assays were carried out as described previously (14) except in the last step, 100 μL of LumiGLO Chemiluminescent Substrate (KPL) was added instead of TMB and stop solution. Samples were developed for 10 minutes and quantified using Synergy H1 Multi-Mode Reader (Biotek).

Downloaded from http://aacrjournals.org/mct/article-pdf/15/5/958/1851970/958.pdf by guest on 24 August 2022

In vitro cytotoxicity assays

Cell lines for cytotoxicity assays were obtained from ATCC, and they were tested for target molecule expression using immunofluorescence and FACS. No further authentication was performed. *In vitro* cytotoxicity studies were carried out as described previously (9, 14). IC_{50} values were calculated by GraphPad Prism 5 software.

In vivo efficacy studies

In vivo efficacy studies were performed using the high target-expressing BxPC3 (M1S1+++) xenograft model. Tumor volume was monitored in female CB17 SCID mice ($n = 5$ per group) following a single injection of 3 mg/kg C16 Site D-Linker 5-VC-PABC-MMAD or 3 mg/kg C16 Site D-Linker 7-VC-PABC-MMAD. A nonbinding antibody conjugate was used as a negative control.

Chemical synthesis

The detailed schemes for chemical synthesis of linker-payloads are provided in Supplementary Methods.

Results and Discussion

Identification of the mouse serum enzyme responsible for the VC-PABC linker cleavage

We previously used several protease inhibitors to probe the enzymatic mechanism responsible for position-dependent cleavage of the C6-VC-PABC-Aur0101 linker-payload in mouse plasma (14). In those studies, the linker-payload conjugated at the cleavage-susceptible Site A was incubated in mouse plasma in the presence of various protease inhibitors, and the amount of intact linker-payload remaining was assessed using HIC or mass spectrometry. The inhibition assays indicated that the enzymatic mechanism involved a serine hydrolase with inhibitor sensitivity distinct from that of the lysosomal cysteine protease CatB, suggesting that the VC-PABC linker degradation in the plasma is not likely due to the activity of extracellular CatB, which has been postulated to be released from some cancerous cells (17–19). Building on those studies, we expanded inhibitor screening to include the inhibitor Bis-para-nitrophenylphosphate (BNPP), known to affect the serine esterase family of enzymes, several of which are known to be present in mammalian blood (20, 21). Using the C16 antibody Site A-C6-VC-PABC-Aur0101 conjugate as a substrate for enzymatic cleavage in mouse plasma, we observed a complete inhibition of the mouse hydrolase in the presence of Pefabloc, a serine protease inhibitor also reported to affect serine esterases, and the esterase inhibitor BNPP (Fig. 1A).

To further characterize and identify the enzyme, we enriched the C6-VC-PABC-Aur0101 linker hydrolysis activity by fractionating the Balb/c mouse serum using a number of biochemical steps. We used an LC/MS-MS method to detect the relative amount of Aur0101 payload released as a way to monitor the VC-PABC hydrolase activity in all fractions. After initial depletion of the Balb/c serum of albumin and immunoglobulins, the sample was subjected to sequential precipitation with ammonium sulfate. Fractions with the highest activity were applied to cation exchange chromatography, followed by anion exchange chromatography, and finally separated by size exclusion chromatography. The highest hydrolase activity fraction eluted around 50–80 kDa (Supplementary Fig. S1), and retained sensitivity to both Pefabloc and BNPP (Fig. 1B). Proteomic analysis of the active fraction identified mouse Carboxylesterases 1C and 1G (Ces1C and Ces1G) among the top candidates, both capable of hydrolyzing amide bonds, and both potentially sensitive to the serine hydrolase inhibitors Pefabloc and BNPP (22). To determine whether Ces1C, Ces1G, or both enzymes can cleave the VC-PABC–based linkers, the activity of commercially available mouse Ces1C and Ces1G, expressed recombinantly from yeast and a mouse myeloma cell line, respectively, was tested with the C16 Site A-C6-VC-PABC-Aur0101 substrate. The assay showed that mouse Ces1C, but not Ces1G, is capable of hydrolyzing the C6-VC-PABC linker. Mass spectrometry confirmed the expected loss of the 873 kDa payload moiety with the purified Ces1C enzyme, which is identical to the cleavage observed in mouse plasma (Supplementary Fig. S2). Furthermore, we showed that the purified mouse Ces1C, but not Ces1G, is capable of cleaving the C-terminal portion of the non-cleavable PEG6-C2-MMAD linker-payload (Supplementary Fig. S3), demonstrating that the same enzyme is involved in the processing of both the VC-PABC linker and the MMAD payload in mouse plasma.

To further verify that the hydrolytic activity of the yeast-expressed Ces1C is not due to the presence of an undefined contaminating protease, we expressed the recombinant protein in the human Expi293 cell line. Following purification using affinity chromatography, a single protein band was observed on SDS-PAGE gel analysis (Fig. 1C). The Expi293-expressed Ces1C protein showed activity towards the C6-VC-PABC-Aur0101 conjugate at levels comparable with the commercial enzyme (data not shown). The fact that both the yeast-expressed and Expi293-expressed versions of Ces1C enzyme retain activity towards the C6-VC-PABC linker provides further evidence for the correct identification of mouse Ces1C as the extracellular linker hydrolase.

To investigate whether Ces1C is the only enzyme responsible for cleaving the VC-PABC–based linkers in mouse serum, we obtained plasma from *Ces1C*$^{-/-}$ knockout mice. The knockout mouse had been originally developed as a model to test various nerve agents that are typically deactivated by Ces1C in the mouse but can have highly toxic effects in other species (23, 24). In contrast to the efficient processing in the *Ces1C*$^{+/+}$ plasma, hydrolysis of the Site A-C6-VC-PABC-Aur0101 conjugate was entirely eliminated in the knockout *Ces1C*$^{-/-}$ mouse plasma assay (Fig. 1D).

While the *in vitro* stability assays are predictive of *in vivo* stability, we previously observed higher linker cleavage activity *in vivo* (14). To find out if only Ces1C is responsible for cleavage of VC-PABC linkers in mouse systemic circulation, we carried out a comparative pharmacokinetic study in *Ces1C*$^{-/-}$ and *Ces1C*$^{+/+}$ mice. The C16 conjugate featuring a modified version of the C6-VC-PABC linker, Linker 1-VC-PABC-Aur0101 (shown in Fig. 2B) coupled to the previously described stable Site F (14) was administered into the animals as a single 6 mg/kg intravenous dose, and the stability of the conjugate in each mouse strain was assessed by comparing total antibody and anti-drug ELISA. There was a significant loss of the Aur0101 payload in the wild-type *Ces1C*$^{+/+}$ animals, resulting in a much lower ADC exposure as compared with the total antibody, whereas the knockout *Ces1C*$^{-/-}$ animals showed no difference between the ADC and total antibody pharmacokinetic profiles (Fig. 1E). This result demonstrates that Ces1C is the primary enzyme responsible for the extracellular cleavage of VC-PABC–based conjugates in mouse.

To evaluate the levels of Ces1C present in mouse serum, we used Western blot analysis to visualize the amount of endogenous

Downloaded from http://aacrjournals.org/mct/article-pdf/15/5/958/1851970/958.pdf by guest on 24 August 2022

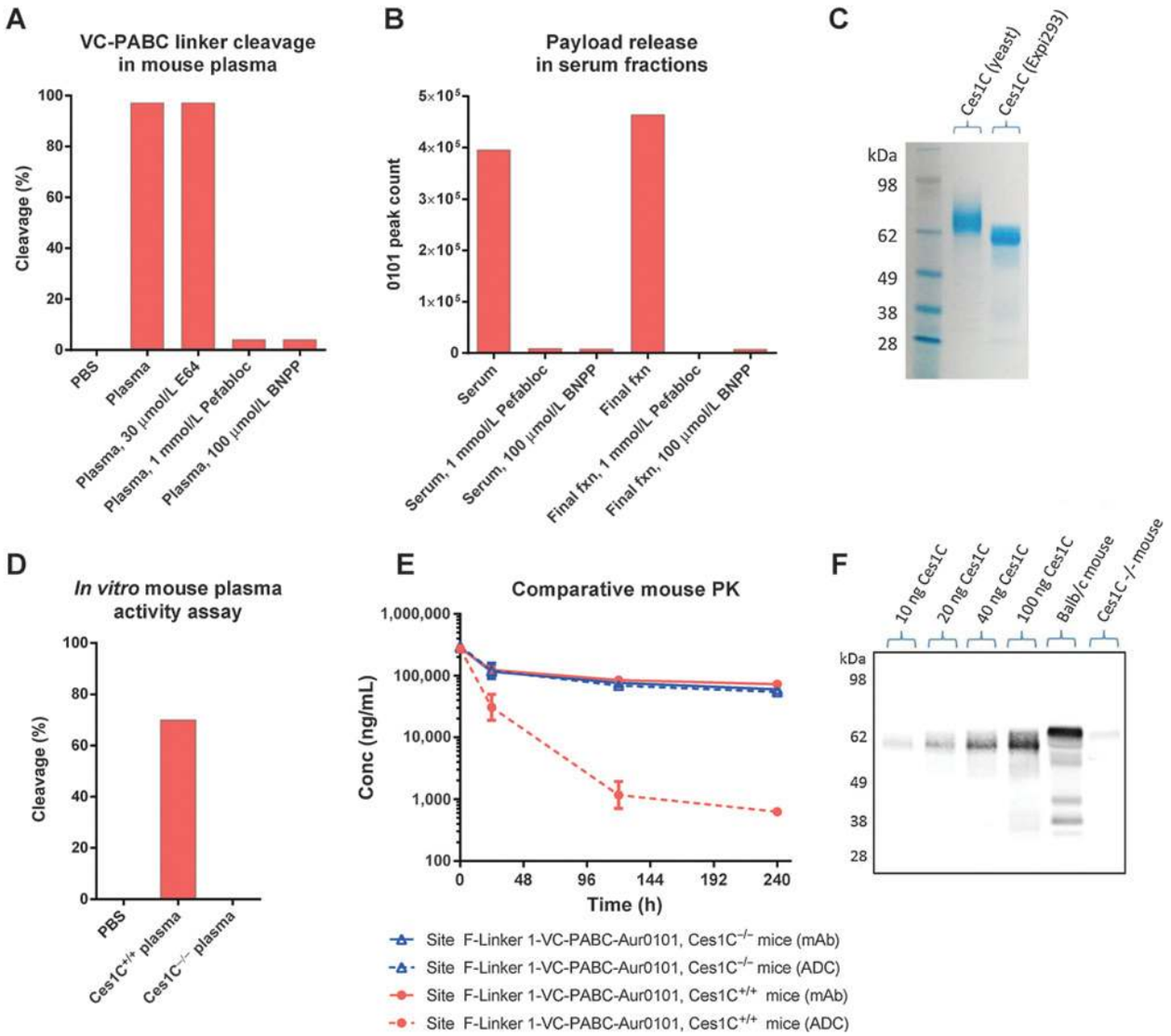

Figure 1.
Identification of the mouse serum enzyme responsible for the VC-PABC linker cleavage. A, hydrolysis of C16 Site A-C6-VC-PABC-Aur0101 conjugate in mouse plasma over 4.5 days, and its inhibition with protease and esterase inhibitors. The graph bars represent percentage of substrate cleaved based on HIC analysis, and are based on several independent measurements. B, evaluation of VC-PABC linker cleavage activity in the starting mouse serum and the final enriched fraction. The relative amount of 0101 payload released from C16 Site A-C6-VC-PABC-Aur0101 after a 50-hour incubation was evaluated using a LC/MS-MS method. C, SDS-PAGE analysis of the purified mouse Ces1C proteins expressed in yeast (MyBioSource) or Expi293 cells (performed in house). Approximately 2 μg of protein loaded per lane. The difference in size is likely due to different glycosylation states of the two proteins generated in different expression systems. D, *in vitro* cleavage of C16 Site A-C6-VC-PABC-Aur0101 conjugate in Ces1C$^{+/+}$ and Ces1C$^{-/-}$ mouse plasma. Duplicate samples incubated for 20 hours were analyzed using HIC. E, *in vivo* pharmacokinetics of C16 Site F-Linker 1-VC-PABC-Aur0101 conjugate dosed into Ces1C$^{+/+}$ and Ces1C$^{-/-}$ mice. The solid lines represent total antibody ELISA, and the dashed lines represent anti-Aur0101 ELISA. F, Western blot analysis of purified mouse Ces1C in comparison with mouse serum. Increasing amounts of purified mouse Ces1C are loaded per lane, along with sera from Balb/c mice, and Ces1C$^{-/-}$ mice. Detection was carried out using polyclonal rabbit anti-mouse Ces1C, followed by IRDye 800 CW-coupled secondary antibody. Quantification using LI-COR Odyssey reveals a unique band of high intensity in the Balb/c serum, but not the Ces1C$^{-/-}$ serum.

Ces1C relative to purified recombinant protein. Previous attempts to quantify plasma levels of Ces1C relied solely on its enzymatic activity compared with an enriched protein (25). We used an anti-mouse Ces1C polyclonal antibody to compare the intensity of the recombinant Ces1C band of known concentration with that of the endogenous protein in the whole Balb/c mouse serum sample (Fig. 1F). The results show that Ces1C is highly abundant in the Balb/c mouse serum with the estimated concentration $\geq$ 80 μg/mL, which correlates with the high VC-PABC linker cleavage rates. As expected, no Ces1C protein was detected in the serum from *Ces1C*$^{-/-}$ knockout mice (Fig. 1F).

The VC-PABC dipeptide linkers constitute the most widely applied cleavable linker modality among ADCs in clinical development, commonly utilizing maleimide chemistry for chemical

Downloaded from http://aacrjournals.org/mct/article-pdf/15/5/958/1851970/958.pdf by guest on 24 August 2022

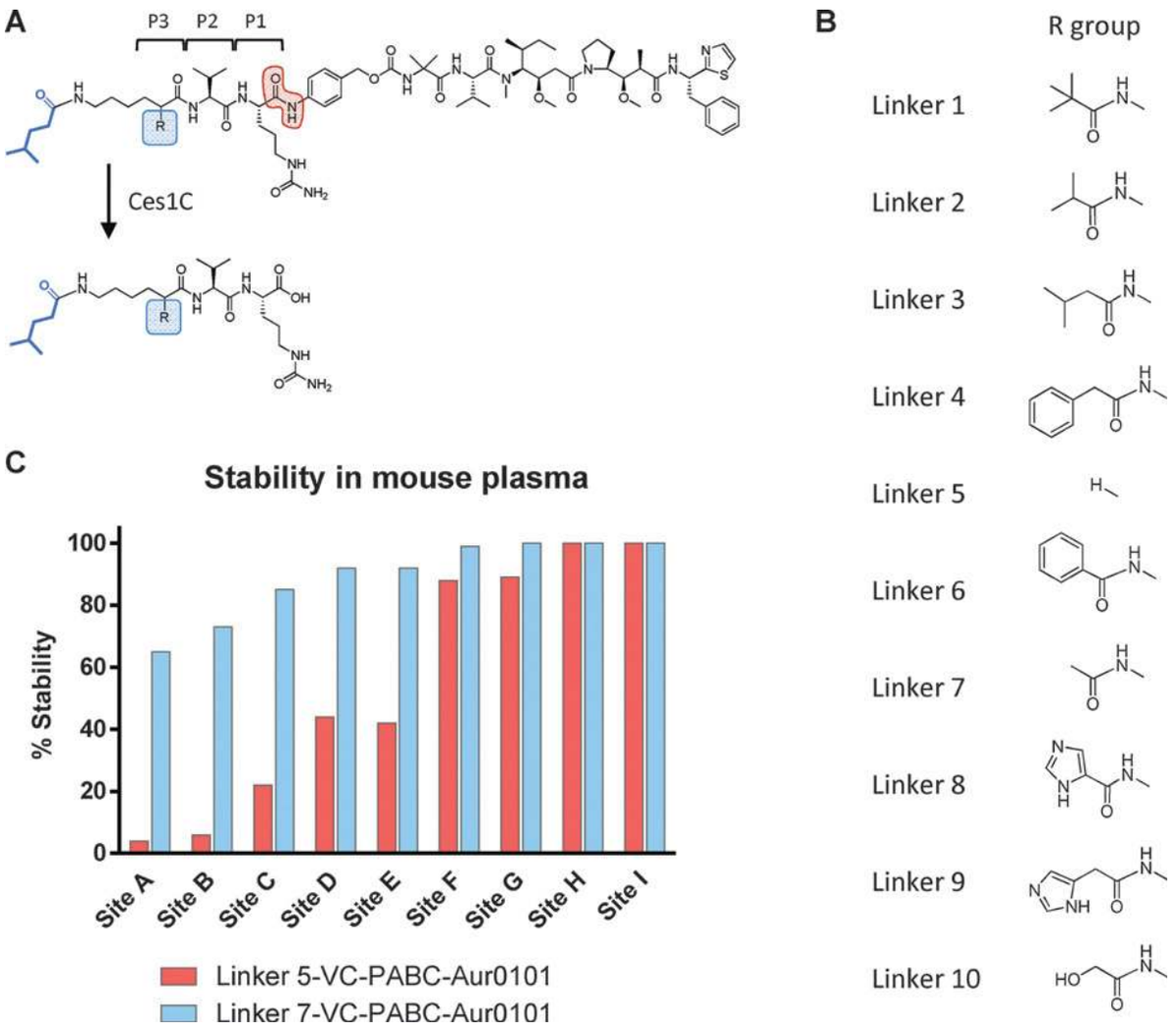

Figure 2.
Modification of VC-PABC cleavable linker and effect on its stability. A, structure of the cleavable C6-VC-PABC-Aur0101 linker-payload conjugated to the glutamine residue on the antibody (in blue), and the C6-VC "stub" remaining following cleavage by mouse Ces1C. The amide bond susceptible to enzymatic cleavage is highlighted in red. The R-group introduced at the C2 position of the aminocaproyl chain within the C6-VC-PABC-Aur0101 linker-payload is highlighted in blue. The substrate residues P1, P2, and P3 are indicated. B, structures of substitutions introduced at the C6-VC-PABC linker described in this study. The R-groups are ranked from conferring the least to the most stability. C, relative mouse plasma stability of Linker 5-VC-PABC-Aur0101 and Linker 7-VC-PABC-Aur0101 conjugated across multiple sites on the C16 antibody. Stability is expressed as percentage of intact conjugate remaining after 4.5-day incubation in mouse plasma. Quantification was carried out using HIC analysis (sites A–F) or mass spectrometry (sites G–I). The conjugates carrying Linker 7-VC-PABC-Aur0101 show consistently higher stability than the corresponding conjugates with Linker 5, with the most pronounced difference between them at the labile site A, and no discernable differences at the protected sites G, H, and I.

coupling to native or engineered cysteines on the antibody. We were interested whether mouse Ces1C can catalyze hydrolysis of the VC-PABC linker in the context of maleimide-coupled conjugates. Analysis of maleimide-linked ADC metabolites after *in vivo* or *in vitro* plasma incubation can be challenging due to the heterogeneous nature of conventional conjugates, as well as maleimide ring opening or maleimide decoupling that can occur in plasma environment (7, 26, 27). We therefore utilized purified mouse Ces1C in the absence of plasma to examine its ability to cleave the maleimide-caproyl-VC-PABC-Aur0101 (mc-VC-PABC-Aur0101) linker-payload chemically coupled to the native cysteines of the C16 antibody (Supplementary Fig. S4A). After incubation of C16-mc-VC-PABC-Aur0101 conjugate with mouse Ces1C at 37°C, mass spectrometry analysis revealed an 875 kDa mass loss for the light chain DAR 1 species (Supplementary Fig. S4C and S4G), and 871 kDa mass loss for the heavy chain DAR 3 species (Supplementary Fig. S4D and S4H), both in agreement with predicted cleavage at the VC-PABC linker (Supplementary Fig. S4A and S4B). No changes in mass spectra were observed for either light chain or heavy chain after incubation at 37°C in buffer alone (Supplementary Fig. S4E and S4F). While we did not aim to quantify the cleavage of the mc-VC-PABC linker by Ces1C, it is possible that it is relatively low for conventional ADCs with high drug loading. Previous studies have shown that VC-PABC linker

Downloaded from http://aacrjournals.org/mct/article-pdf/15/5/958/1851970/958.pdf by guest on 24 August 2022

Table 1. *In vitro* stability of linker-payload variants in plasma from different species

Site	Position	Linker-payload	Mouse plasma stability (%)	Rat plasma stability (%)	Cyno plasma stability (%)
A	LC 200–202	Linker 1-VC-PABC-Aur0101	0	48	95
A	LC 200–202	Linker 2-VC-PABC-Aur0101	0	75	95
A	LC 200–202	Linker 4-VC-PABC-Aur0101	0	83	96
A	LC 200–202	Linker 5-VC-PABC-Aur0101 (C6)	5	94	99
A	LC 200–202	Linker 6-VC-PABC-Aur0101	6	95	98
A	LC 200–202	Linker 7-VC-PABC-Aur0101	65	96	97
A	LC 200–202	Linker 8-VC-PABC-Aur0101	67	94	95
A	LC 200–202	Linker 9-VC-PABC-Aur0101	62	97	100
A	LC 200–202	Linker 10-VC-PABC-Aur0101	84	97	100
F	LC C-terminus	Linker 1-VC-PABC-Aur0101	9	91	99
F	LC C-terminus	Linker 2-VC-PABC-Aur0101	49	92	100
F	LC C-terminus	Linker 3-VC-PABC-Aur0101	61	95	100
F	LC C-terminus	Linker 4-VC-PABC-Aur0101	71	96	99
F	LC C-terminus	Linker 5-VC-PABC-Aur0101 (C6)	86	99	100
F	LC C-terminus	Linker 6-VC-PABC-Aur0101	95	98	100
F	LC C-terminus	Linker 7-VC-PABC-Aur0101	99	99	100
F	LC C-terminus	Linker 8-VC-PABC-Aur0101	94	95	95
F	LC C-terminus	Linker 9-VC-PABC-Aur0101	97	98	99

NOTE: VC-PABC linker-payload variants conjugated at either Site A or Site F of C16 antibody were tested for stability in plasma from mouse, rat, and cynomolgus monkey. Stability values are based on HIC analysis of the percent of intact conjugate remaining after a 4.5-day incubation in plasma.

Downloaded from http://aacrjournals.org/mct/article-pdf/15/5/958/1851970/958.pdf by guest on 24 August 2022

stability depends on the conjugation site, where neighboring antibody domains might be shielding the linker from the enzyme (13, 14). Additional protection from cleavage could be conferred by the adjacent payload moieties which might be arranged more closely to each other in high loaded site-specific or conventional conjugates.

Modifications of the VC-PABC linker and their effect on conjugate stability and efficacy

The identification of Ces1C as the enzyme responsible for the instability of VC-PABC linkers in rodent plasma prompted us to explore ways to modify the VC-PABC linker to eliminate the Ces1C sensitivity while preserving susceptibility towards CatB and other lysosomal proteases. Mitigating ADC instability in rodent systemic circulation is a prerequisite for proper evaluation of safety and efficacy in preclinical studies that utilize mouse and rat species.

A number of VC-PABC linker modifications were designed by introducing chemical modifications on the linker position immediately preceding the valine residue, that is, the P3 position upstream of the enzymatic cleavage site (Fig. 2A). These initial selections were chosen to explore relatively small hydrophobic substituents that varied in steric bulk, with a few select cases including introduction of polar functionality. In the previously described transglutaminase-based conjugation method, this amino acid position typically harbors the primary amine-containing group, such as the aminocaproyl chain, which can participate in the transamidation reaction to form a covalent bond with the γ-carboxamide group of the glutamine residue on the antibody (Fig. 2A; refs.13, 28).

Several chemical groups were introduced at the C2 position of the C6-VC-PABC-Aur0101 linker-payload (Fig. 2B), followed by conjugation to one of the aforementioned sites on the C16 antibody. We previously showed that the extent of VC-PABC linker cleavage in rodent plasma could vary greatly depending on the site of conjugation, with some sites conferring high level of protection from cleavage, possibly due to steric shielding from Ces1C by the antibody domains (14). In comparative plasma stability assays, the C6-VC-PABC-Aur0101 linker-payload (Linker 5-VC-PABC-Aur0101) showed consistently lower stability across all conjugation sites than Linker 7-VC-PABC-Aur0101 with acetylamino group introduced at the C2 position (Fig. 2B and C). The stability difference between Linker 5 and Linker 7 conjugates was the most evident at the least protected Sites A and B, while the more shielded Sites H and I allowed high levels of plasma stability for both linkers (Fig. 2C).

To examine whether the VC-PABC cleavage rates might depend on linker chemistry, we tested an entire panel of VC-PABC linker-payload derivatives (Fig. 2B) conjugated to the least stable Site A or the more stable Site F on the C16 antibody. In addition to a single time point measurement across all the linker-payload conjugates in plasma from different species (Table 1), we also carried out a time course of selected conjugates in Balb/c mouse plasma (Fig. 3A and 3D). The data shows a wide range of VC-PABC linker cleavage rates in mouse plasma (Table 1; Fig. 3A and D), and a lower degree of instability is detected in the rat and cynomolgus monkey plasma (Table 1).

Similarly to *in vitro* mouse plasma assays, in comparative enzymatic assays, selected linker-payload derivatives conjugated at Site A showed distinct degrees of susceptibilities to the purified Ces1C, with Site A-Linker 1-VC-PABC-Aur0101 being hydrolyzed much more rapidly than the Site A-Linker 5-VC-PABC-Aur0101 conjugate, and Site A-Linker 10-VC-PABC-Aur0101 was almost entirely inert to degradation over the course of the assay (Fig. 3A and B). Although the range of hydrolysis rates is much narrower among the different VC-PABC linker derivatives on the more protected Site F, all the linkers show the same stability ranking as seen at Site A (Table 1; Fig. 3D and E). These results demonstrate that regardless of the conjugation site on the antibody, linker modification described in this study offers an orthogonal method for modulating ADC stability in rodents, allowing for VC-PABC linker stabilization even at the most susceptible sites. Development of Ces1C-resistant linkers provides a way to conjugate payloads at a wider range of positions across the antibody as it alleviates the dependence on steric protection (alone) of the linker-payload by the antibody domains.

For proper ADC function, it is essential that the antibody–drug linkage remains stable in plasma, but can still be efficiently

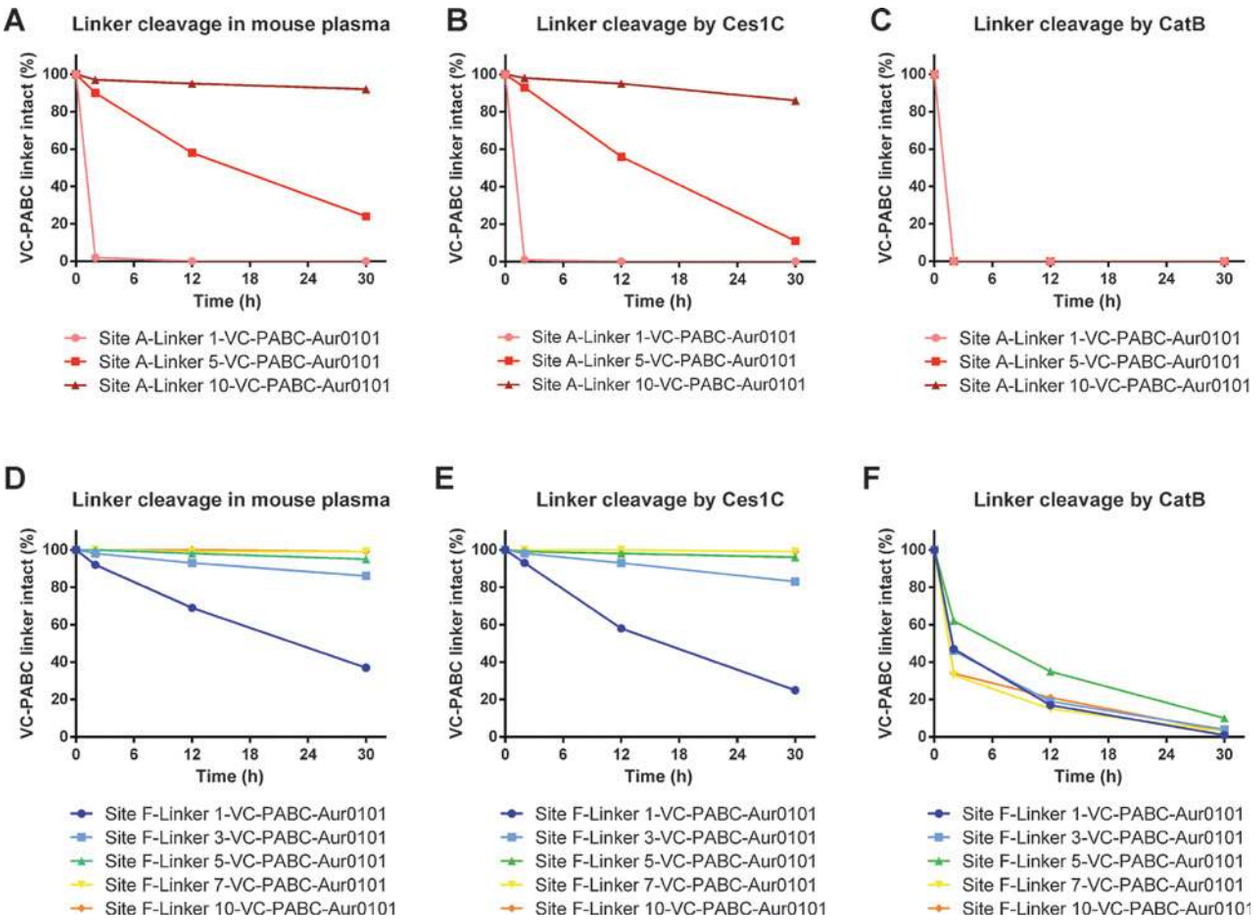

Figure 3.

Comparison of enzymatic cleavage of derivatized VC-PABC linkers by extracellular Ces1C and intracellular CatB. Processing of selected modified linker-payload conjugates in mouse plasma (A and D) or with purified mouse Ces1C at 40 μg/mL (B and E) and human liver CatB at 0.5 μg/mL (C and F) over a 30-hour incubation. Different linker-payload derivatives conjugated at the labile Site A show distinct processing rates in the context of mouse plasma (A), and in the presence of mouse Ces1C (B), but are all readily cleaved by lysosomal CatB (C). Linker modification within the more protected Site F conjugates can still significantly contribute to differential susceptibility to cleavage in mouse plasma (D) or by purified Ces1C (E). Cleavage of Site F conjugates by CatB is slower as compared with Site A conjugates, but the differences between linker derivatives are small (F).

processed upon internalization. To test whether the described linker derivatives can undergo intracellular processing by the lysosomal protease CatB, we set up enzymatic activity assays using human and mouse CatB. All tested linker-payloads conjugated at Site A were readily cleaved by CatB at very comparable rates under the conditions of our assay (Fig. 3C), suggesting that this enzyme does not discriminate among VC-PABC linker substitutions. The degree of cleavage was also comparable among the tested linker derivatives conjugated at Site F, although the hydrolysis of all linker-payloads by CatB was slower than at Site A (Fig. 3F). These observations indicate that while VC-PABC linkers attached at Site F might be shielded to some extent from degradation by CatB through steric hindrance by the adjacent antibody domains, the chemical identity of the linker substitution itself plays a minimal role in determining the hydrolytic activity of CatB. In other words, all substitutions explored on these sites that displayed a wide range of susceptibilities toward cleavage by Ces1C, showed very comparable sensitivity toward hydrolysis by CatB. This suggests that modifications at or near the P3 substrate residue have minimal effects on substrate recognition by CatB, but allow for a high degree of substrate discrimination by Ces1C. We postulate that these differences in substrate selectivity by the two enzymes are, in part, due to the distinct characteristics of their substrate-binding pockets. While currently there is no known structure of mouse Ces1C available, the homologous structure of human liver carboxylesterase (29) shows that the catalytic serine residue of mammalian carboxylesterase is positioned deep within a narrow elongated pocket (Fig. 4A). Distinct patterns of substrate selectivity have been reported for several human carboxylesterases, where the unique positioning of the functional groups of the substrate within the rigid and flexible binding pockets of the enzyme can contribute to drastically different rates of hydrolysis (30, 31). The complexity of this deep binding site cavity likely contributes to the high degree of substrate selectivity, allowing mouse Ces1C to distinguish between the various VC-PABC linker substitutions. The deep positioning of the catalytic Ser residue within Ces1C also suggests that the payload attached to the VC-PABC linker will be in contact with the enzyme and

Downloaded from http://aacrjournals.org/mct/article-pdf/15/5/958/1851970/958.pdf by guest on 24 August 2022

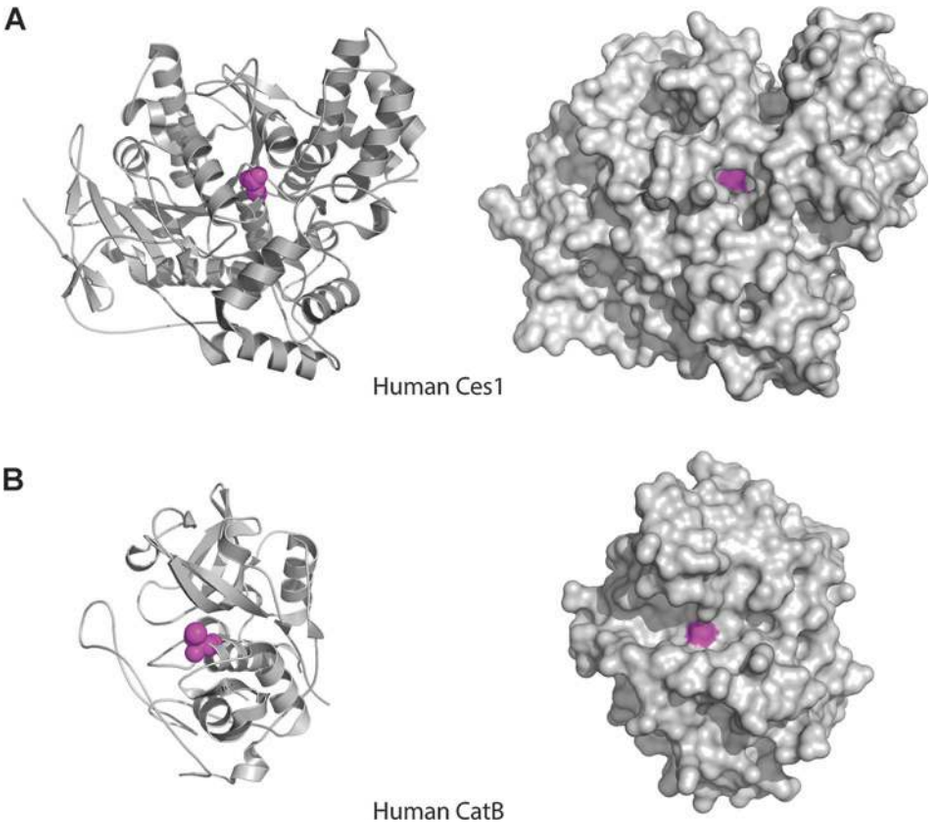

Figure 4.
Structural comparison of human liver carboxylesterase and lysosomal CatB. A, crystal structure of human liver carboxylesterase (PDB 1MX1) showing the ribbon model (left) and space filling model (right). The active site serine shown in magenta is located deep within the substrate binding pocket. B, crystal structure of human liver CatB (PDB 1HUC) showing the ribbon model (left) and space filling model (right). The reactive cysteine shown in magenta resides in a more shallow substrate binding site, likely allowing for a high degree of tolerance towards the substrate P3 residue. The difference in the active site accessibility is likely to contribute to the differences in substrate selectivity of the two enzymes.

might also influence the cleavage of the linker. The sensitivity to linker chemistry is unlikely to be the case for lysosomal CatB which has a shallow active site that is more accessible by diverse substrates, which gives rise to its promiscuity (Fig. 4B). On the basis of the structure of human CatB (32), the modifications at the P3 substrate residue are likely positioned near the edge or outside of the CatB binding pocket, which can explain why they have little effect on the VC-PABC cleavage rates by CatB (Fig. 3C and 3F). This basic difference in the architecture of the Ces and CatB active sites might be a key contributor to the drastically distinct levels of substrate discrimination by the two enzymes: extracellular Ces1C is able to distinguish among these VC-PABC linker derivatives, while lysosomal CatB hydrolyzes all derivatives at very similar rates. Future work will focus on expanding our structural knowledge of mouse Ces1C and its interactions with a broad range of VC-PABC-Aur0101 substrates to elucidate understanding of substrate interactions at the molecular level, and possible differences between the mouse and human homologs.

We note that in the context of the lysosome, the processing of VC-PABC–based linkers by CatB might be further facilitated by the presence of other proteases and denaturing factors. In fact, all C16 Site F linker-payload derivatives showed similar potency in cytotoxicity assays against the target-expressing BxPC3 pancreatic cancer cell line (Supplementary Fig. S5A) suggesting an efficient intracellular payload release from all derivatives irrespective of the type of modification introduced. Target specificity was confirmed by lack of efficacy against non-expressing SW620 cell line (Supplementary Fig. S5B). These observations highlight the important finding that derivatization of the VC-PABC linker in site-specific cleavable conjugates can provide an effective protection from the extracellular cleavage by Ces1C in rodent plasma without interfering with the intracellular processing of the linkers in the lysosome hydrolytic pathway of the target cell. In mouse, we can therefore modulate the rates of extracellular payload release from the VC-PABC-linker derivatives while maintaining efficient intracellular payload processing.

We previously showed a correlation between plasma stability of conjugates with Linker 5-VC-PABC-Aur0101 attached at different positions of the antibody and their efficacy *in vitro* and *in vivo* (14). To test whether exposure to mouse plasma could reduce cytotoxic potency of the conjugates with linker-payload modifications, we preincubated selected derivatized conjugates in plasma for 4.5 days, and compared their cytotoxicity to the starting material. Preincubation in mouse plasma reduced potency of the conjugate with the least stable Linker 1 (Supplementary Fig. S5C), but had a much smaller effect on conjugate with more stable Linker 4 (Supplementary Fig. S5D), and no effect on conjugate with Linker 9, which remains mostly intact during the course of preincubation (Supplementary Fig. S5E).

To determine whether linker derivatization can also modulate conjugate stability *in vivo*, we carried out pharmacokinetic studies in SCID mice which carry the wild-type *Ces1C*$^{+/+}$ genotype. Selected compounds were administered as a single 9 mg/kg intravenous dose, and plasma samples were analyzed using total antibody and anti-drug ELISA assays. The total antibody exposure was essentially identical for all tested conjugates demonstrating

Downloaded from http://aacrjournals.org/mct/article-pdf/15/5/958/1851970/958.pdf by guest on 24 August 2022

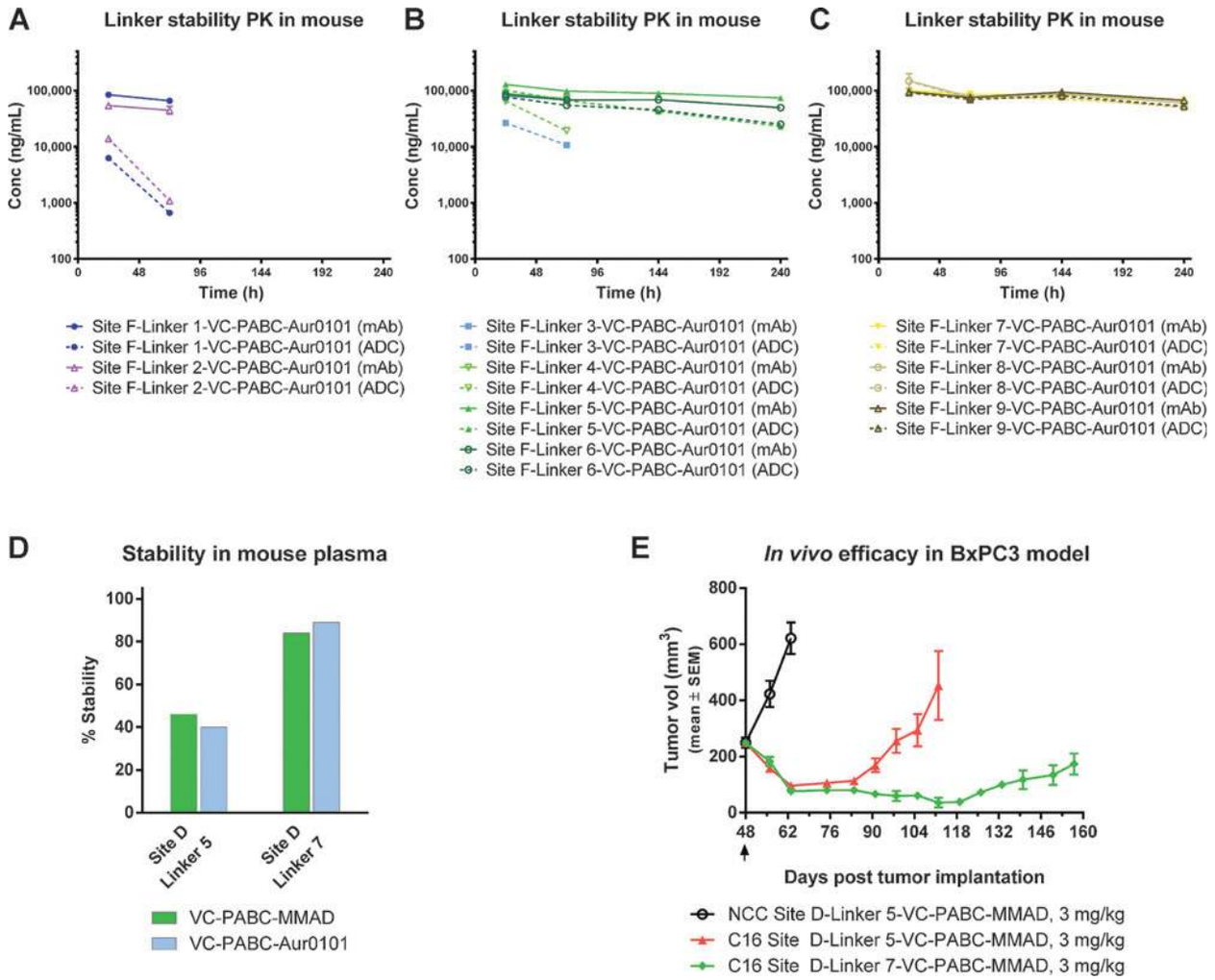

Figure 5.

Stability and efficacy of VC-PABC–based conjugates *in vivo*. A–C, pharmacokinetic profiles of Site F-conjugated linker-payload derivatives in SCID mice. After a single dose of 9 mg/kg, total antibody ELISA (solid lines) and anti-Aur0101 ELISA (dashed lines) revealed distinct rates of payload loss among conjugates with different VC-PABC linker modifications. On the basis of these differences, linker-payloads were grouped into least stable (A), intermediate (B), and most stable (C), which reflected their stabilities observed *in vitro*. D, comparison of linker stability dependence on the linker chemistry for VC-PABC-MMAD (green) and VC-PABC-Aur0101 (blue) conjugates. The two payloads attached through either Linker 5 or Linker 7 to Site D of the C16 antibody were incubated in mouse plasma for 4.5 days. Stability is expressed as percentage of intact conjugate remaining, and quantification was carried out using HIC analysis. E, comparative *in vivo* efficacy of Linker 5-VC-PABC-MMAD and Linker 7-VC-PABC-MMAD conjugated to the intermediate stability Site D. Conjugates were tested in the BxPC3 pancreatic xenograft model in SCID mice, following a single 3 mg/kg dose. A nonbinding conjugate with Linker 5-VC-PABC-MMAD was included as a negative control.

good overall pharmacokinetic stability (Fig. 5 A–C). However, the rates of VC-PABC cleavage and payload release from the different linker derivatives showed considerable variation that was consistent with their relative susceptibilities to extracellular Ces1C cleavage. Similar to the *in vitro* results, we observed linkers with rapid loss of payload (Fig. 5A), intermediate loss of payload (Fig. 5B), and very slow release of payload (Fig. 5C). This slow release of payload resulted in high ADC exposure over the course of 10 days after injection for the most stable conjugates.

The effect of linker-payload stability in mouse circulation on conjugate efficacy *in vivo* was also demonstrated using two C16 antibody conjugates carrying a related MMAD payload attached through two different linkers. We first carried out a comparative mouse plasma stability assay to demonstrate that VC–PABC–MMAD conjugates show similar susceptibility to Ces1C hydrolysis as VC-PABC-Aur0101 conjugates (Fig. 5D). Using Linker 5-VC-PABC-MMAD and Linker 7-VC-PABC-MMAD attached to Site D of the C16 antibody, and the equivalent Linker 5-VC-PABC-Aur0101 and Linker 7-VC-PABC-Aur0101 attached to the same site, we observe a similar dependence of linker stability on the chemical modification of the linker in the context of both payloads (Fig. 5D). To test the effect of linker degradation on *in vivo* efficacy, SCID mice implanted with BxPC3 tumor cells were given a single 3 mg/kg injection of either C16 Site D-Linker 5-VC-PABC-MMAD or C16 Site D-Linker 7-VC–PABC–MMAD conjugate. Both drugs resulted in a significant tumor

Downloaded from http://aacrjournals.org/mct/article-pdf/15/5/958/1851970/958.pdf by guest on 24 August 2022

reduction over an extended period of time (Fig. 5E). However, the rate of tumor regrowth was considerably faster for the less stable Linker 5 conjugate than for the more stable Linker 7. These observations highlight the importance of systemic ADC stability for antitumor efficacy *in vivo*. Previous studies demonstrated the improved efficacy of conjugates wherein the linker-payload protection from extracellular cleavage in mouse plasma was conferred by the conjugation site on the antibody (14). In this study, the linker-payload stabilization is achieved through selected chemical substitutions at the P3 position of the VC-PABC linker, providing resistance to Ces1C hydrolysis even at the least protected conjugation sites. This approach opens up a wider repertoire of positions available for conjugation, and allows for fine tuning of ADC pharmacokinetics in rodents, without affecting the efficiency of intracellular processing and payload potency.

Interspecies differences in VC-PABC linker cleavage by plasma carboxylesterase

Systemic stability of antibody–drug conjugates is one of the key features influencing pharmacokinetic properties and antitumor effectiveness of this class of therapeutics. Degradation of ester, thioester, and amide linkages by the mouse and rat serum carboxylesterases has been reported for a wide range of compounds, including various organophosphates, nerve agents, xenobiotics, prodrugs, and certain ADCs (33–38). The stability of VC-PABC–based cleavable conjugates in the plasma varies greatly among different species. While the mouse plasma Ces1C exhibits high reactivity towards the labile VC-PABC linker derivatives, lower levels of linker cleavage are observed in rat plasma (Table 1; Supplementary Fig. S6A). A similar species dependence has also been observed for the C-terminal degradation of the noncleavable PEG6-C2-MMAD which can occur in the mouse (in a site-dependent manner), and to a lower extent in the rat (Supplementary Fig. S6B; ref. 9). In rat plasma, the VC-PABC linker degradation is also inhibited by the esterase inhibitor BNPP (data not shown) indicating that the cleavage mechanism likely involves rat carboxylesterase.

In an earlier study, we examined the properties of one of the more stable Site F-Linker 7-VC-PABC-MMAD conjugates, and described its comparable *in vivo* PK profiles in both mouse and rat, and somewhat lower VC-PABC cleavage rates in the rat than in mouse based on stability analysis after conjugate purification (13). In the same study, we also examined Site D-Linker 7-VC-PABC-MMAD conjugate in mouse and rat which showed distinct *in vivo* pharmacokinetic profiles, and large differences in the amounts of VC-PABC cleavage products (DAR 0, DAR 1, and DAR 2; ref. 13). While we observed accumulation of the DAR 1 metabolite in rat plasma, it was largely absent in mouse plasma, suggesting that the single drug-loaded conjugate can be cleaved relatively rapidly in the mouse, but is more stable in the rat (13) consistent with our recent data (Supplementary Fig. S6; ref. 14). The rapid loss of the DAR 2 species in the rat, which is specific to Site D (13), is likely due to a preferential rapid clearance of the DAR 2 from the blood compartment rather than due to high activity of rat carboxylesterase. In fact, it has been reported that the hydrophobicity of the conjugated payloads, and their positioning play a significant role in the *in vivo* distribution and degradation of ADCs (39, 40).

Although linker cleavage is essentially undetectable in cynomolgus monkey and human plasma (Table 1; Supplementary Fig. S6A), some degree of payload release was observed in an *in vivo* cynomolgus monkey pharmacodynamic study after dosing with a Site D-Linker 5-VC-PABC-MMAD conjugate (14). However, it could not be determined whether the loss of payload was due to an enzymatic activity in the monkey plasma or another *in vivo* process such as endosomal recycling. It has been unclear whether human plasma might contain any carboxylesterase homologs. Earlier findings attributed some *p*-nitrophenyl acetate reactivity in human plasma to the presence of carboxylesterase (33, 41); however, more recent studies report no carboxylesterase found in human plasma (25). It is possible that carboxylesterase might be present at a very low concentration range in the primates, similar to acetylcholinesterase levels, but be induced or secreted into the plasma under certain conditions. In addition, in our assays neither human liver carboxylesterase nor human intestinal carboxylesterase were capable of hydrolyzing VC-PABC–linked ADCs (data not shown). This result suggests an inherent lack of reactivity of the human enzymes towards VC-PABC–based substrates, and might be due to subtle differences within the active site of the mouse Ces1C and its human homologs.

Thanks to the substrate selectivity of the mouse Ces1C, we can design VC-PABC linker modifications that will make preclinical studies of ADC more comparable among species by eliminating the exposure differences caused by VC-PABC linker cleavage in mouse. Because of the divergent substrate specificity of Ces1C and lysosomal CatB, we can minimize the loss of payload in circulation while keeping the intracellular processing necessary for ADC activity unchanged. Modulating the extracellular stability of VC-PABC–based ADCs using linker chemistry is an orthogonal yet complementary approach to the previously described selection of conjugation sites (13, 14), allowing for stabilization of linker-payloads even at the highly exposed and least protected positions on the antibody. Combination of site selection and choice of stable linker can have an additive effect that can generate ADCs that are highly stable in plasma, yet retain their activity towards target cancer cells. Furthermore, the VC-PABC linker derivatives can be easily utilized for controlling the pharmacokinetic release of cytotoxic payload to study the effects of ADC exposure on efficacy and toxicity in rodent models.

Disclosure of Potential Conflicts of Interest

R. Dushin has ownership interest in stock and stock options in Pfizer, Inc. J. Pons has ownership interest (including patents) in Pfizer. D.L. Shelton has ownership interest (including patents) in Pfizer. No potential conflicts of interest were disclosed by the other authors.

Authors' Contributions

Conception and design: M. Dorywalska, R. Dushin, L. Moine, C.J. O'Donnell, J. Pons, A. Rajpal, P. Strop

Development of methodology: M. Dorywalska, L. Moine, S.E. Farias, D. Zhou, T. Navaratnam, A. Hasa-Moreno, K. Delaria, P. Strop

Acquisition of data (provided animals, acquired and managed patients, provided facilities, etc.): M. Dorywalska, S.E. Farias, V. Lui, A. Hasa-Moreno, M.G. Casas, T.-T. Tran

Analysis and interpretation of data (e.g., statistical analysis, biostatistics, computational analysis): M. Dorywalska, D. Zhou, V. Lui, A. Hasa-Moreno, D. Foletti, P. Strop

Writing, review, and/or revision of the manuscript: M. Dorywalska, R. Dushin, S.E. Farias, S.-H. Liu, D. Foletti, C.J. O'Donnell, J. Pons, D.L. Shelton, A. Rajpal, P. Strop

Downloaded from http://aacrjournals.org/mct/article-pdf/15/5/958/1851970/958.pdf by guest on 24 August 2022

Administrative, technical, or material support (i.e., reporting or organizing data, constructing databases): M. Dorywalska, D. Zhou, T. Navaratnam
Study supervision: M. Dorywalska, R. Dushin, D.L. Shelton, A. Rajpal, P. Strop

Acknowledgments

The authors thank German Vergara, Theresa Radcliffe, and Cindy Li for establishing and maintaining the colony of *Ces1C*$^{-/-}$ mice; Colleen Brown for cell culture support; Janette Sutton, Gary Bolton, and Stellanie Krimm for help with *in vivo* studies; Caroline Samain and Dan McDonough for assistance with ELISA analysis; and Mathias Rickert for helpful discussions and chromatography support.

The costs of publication of this article were defrayed in part by the payment of page charges. This article must therefore be hereby marked *advertisement* in accordance with 18 U.S.C. Section 1734 solely to indicate this fact.

Received December 30, 2015; revised February 12, 2016; accepted February 12, 2016; published OnlineFirst March 4, 2016.

References

1. Sievers EL, Senter PD. Antibody-drug conjugates in cancer therapy. Annu Rev Med 2013;64:15–29.
2. Panowksi S, Bhakta S, Raab H, Polakis P, Junutula JR. Site-specific antibody drug conjugates for cancer therapy. MAbs 2014;6:34–45.
3. Ducry L, Stump B. Antibody-drug conjugates: linking cytotoxic payloads to monoclonal antibodies. Bioconjug Chem 2010;21:5–13.
4. Doronina SO, Toki BE, Torgov MY, Mendelsohn BA, Cerveny CG, Chace DF, et al. Development of potent monoclonal antibody auristatin conjugates for cancer therapy. Nat Biotechnol 2003;21:778–84.
5. Sanderson RJ, Hering MA, James SF, Sun MM, Doronina SO, Siadak AW, et al. In vivo drug-linker stability of an anti-CD30 dipeptide-linked auristatin immunoconjugate. Clin Cancer Res 2005;11:843–52.
6. Alley SC, Benjamin DR, Jeffrey SC, Okeley NM, Meyer DL, Sanderson RJ, et al. Contribution of linker stability to the activities of anticancer immunoconjugates. Bioconjug Chem 2008;19:759–65.
7. Shen BQ, Xu K, Liu L, Raab H, Bhakta S, Kenrick M, et al. Conjugation site modulates the in vivo stability and therapeutic activity of antibody-drug conjugates. Nat Biotechnol 2012;30:184–9.
8. Tumey LN, Rago B, Han X. In vivo biotransformations of antibody-drug conjugates. Bioanalysis 2015;7:1649–64.
9. Dorywalska M, Strop P, Melton-Witt JA, Hasa-Moreno A, Farias SE, Galindo Casas M, et al. Site-Dependent degradation of a non-cleavable auristatin-based linker-payload in rodent plasma and its effect on ADC efficacy. PLoS One 2015;10:e0132282.
10. Dubowchik GM, Firestone RA, Padilla L, Willner D, Hofstead SJ, Mosure K, et al. Cathepsin B-labile dipeptide linkers for lysosomal release of doxorubicin from internalizing immunoconjugates: model studies of enzymatic drug release and antigen-specific in vitro anticancer activity. Bioconjug Chem 2002;13:855–69.
11. Doronina SO, Bovee TD, Meyer DW, Miyamoto JB, Anderson ME, Morris-Tilden CA, et al. Novel peptide linkers for highly potent antibody-auristatin conjugate. Bioconjug Chem 2008;19:1960–3.
12. Junutula JR, Raab H, Clark S, Bhakta S, Leipold DD, Weir S, et al. Site-specific conjugation of a cytotoxic drug to an antibody improves the therapeutic index. Nat Biotechnol 2008;26:925–32.
13. Strop P, Liu SH, Dorywalska M, Delaria K, Dushin RG, Tran TT, et al. Location matters: site of conjugation modulates stability and pharmacokinetics of antibody drug conjugates. Chem Biol 2013;20:161–7.
14. Dorywalska M, Strop P, Melton-Witt JA, Hasa-Moreno A, Farias SE, Galindo Casas M, et al. Effect of attachment site on stability of cleavable antibody drug conjugates. Bioconjug Chem 2015;26:650–9.
15. Jeger S, Zimmermann K, Blanc A, Grunberg J, Honer M, Hunziker P, et al. Site-specific and stoichiometric modification of antibodies by bacterial transglutaminase. Angew Chem Int Ed Engl 2010;49:9995–7.
16. Farias SE, Strop P, Delaria K, Galindo Casas M, Dorywalska M, Shelton DL, et al. Mass spectrometric characterization of transglutaminase based site-specific antibody-drug conjugates. Bioconjug Chem 2014;25:240–50.
17. Mohamed MM, Sloane BF. Cysteine cathepsins: multifunctional enzymes in cancer. Nat Rev Cancer 2006;6:764–75.
18. Vasiljeva O, Reinheckel T, Peters C, Turk D, Turk V, Turk B. Emerging roles of cysteine cathepsins in disease and their potential as drug targets. Curr Pharm Des 2007;13:387–403.
19. Reiser J, Adair B, Reinheckel T. Specialized roles for cysteine cathepsins in health and disease. J Clin Invest 2010;120:3421–31.
20. Tomic S, Trescec A, Tomasic J, Petrovic B, Rudolf VS, Skrinjaric-Spoljar M, et al. Catalytic properties of rabbit serum esterases hydrolyzing esterified monosaccharides. Biochim Biophys Acta 1995;1251:11–6.
21. Main AR.Kinetic and structural relationships of transition monomeric and oligomeric carboxyl- and choline-esterases. J Environ Sci Health B 1983;18:29–63.
22. Hatfield MJ, Potter PM. Carboxylesterase inhibitors. Expert Opin Ther Pat 2011;21:1159–71.
23. Duysen EG, Koentgen F, Williams GR, Timperley CM, Schopfer LM, Cerasoli DM, et al. Production of ES1 plasma carboxylesterase knockout mice for toxicity studies. Chem Res Toxicol 2011;24:1891–8.
24. Duysen EG, Cashman JR, Schopfer LM, Nachon F, Masson P, Lockridge O. Differential sensitivity of plasma carboxylesterase-null mice to parathion, chlorpyrifos and chlorpyrifos oxon, but not to diazinon, dichlorvos, diisopropylfluorophosphate, cresyl saligenin phosphate, cyclosarin thiocholine, tabun thiocholine, and carbofuran. Chem Biol Interact 2012;195:189–98.
25. Li B, Sedlacek M, Manoharan I, Boopathy R, Duysen EG, Masson P, et al. Butyrylcholinesterase, paraoxonase, and albumin esterase, but not carboxylesterase, are present in human plasma. Biochem Pharmacol 2005;70:1673–84.
26. Tumey LN, Charati M, He T, Sousa E, Ma D, Han X, et al. Mild method for succinimide hydrolysis on ADCs: impact on ADC potency, stability, exposure, and efficacy. Bioconjug Chem 2014;25:1871–80.
27. Lyon RP, Setter JR, Bovee TD, Doronina SO, Hunter JH, Anderson ME, et al. Self-hydrolyzing maleimides improve the stability and pharmacological properties of antibody-drug conjugates. Nat Biotechnol 2014;32:1059–62.
28. Strop P, Dorywalska M, Rajpal A, Shelton DL, Liu S-H, Pons J, et al. inventors; Pfizer, Rinat Neuroscience Corporation, assignee. Engineered polypeptide conjugates and methods for making thereof using transglutaminase . Patent WO2012059882; 2012 May 10.
29. Bencharit S, Morton CL, Hyatt JL, Kuhn P, Danks MK, Potter PM, et al. Crystal structure of human carboxylesterase 1 complexed with the Alzheimer's drug tacrine: from binding promiscuity to selective inhibition. Chem Biol 2003;10:341–9.
30. Bencharit S, Morton CL, Xue Y, Potter PM, Redinbo MR. Structural basis of heroin and cocaine metabolism by a promiscuous human drug-processing enzyme. Nat Struct Biol 2003;10:349–56.
31. Bencharit S, Edwards CC, Morton CL, Howard-Williams EL, Kuhn P, Potter PM, et al. Multisite promiscuity in the processing of endogenous substrates by human carboxylesterase 1. J Mol Biol 2006;363:201–14.
32. Musil D, Zucic D, Turk D, Engh RA, Mayr I, Huber R, et al. The refined 2.15 A X-ray crystal structure of human liver cathepsin B: the structural basis for its specificity. EMBO J 1991;10:2321–30.
33. Kaliste-Korhonen E, Tuovinen K, Hanninen O. Interspecies differences in enzymes reacting with organophosphates and their inhibition by paraoxon in vitro. Hum Exp Toxicol 1996;15:972–8.
34. Satoh T, Hosokawa M. Structure, function and regulation of carboxylesterases. Chem Biol Interact 2006;162:195–211.
35. Crow JA, Borazjani A, Potter PM, Ross MK. Hydrolysis of pyrethroids by human and rat tissues: examination of intestinal, liver and serum carboxylesterases. Toxicol Appl Pharmacol 2007;221:1–12.
36. Hosokawa M.Structure and catalytic properties of carboxylesterase isozymes involved in metabolic activation of prodrugs. Molecules 2008;13:412–31.
37. Dokter W, Ubink R, van der Lee M, van der Vleuten M, van Achterberg T, Jacobs D, et al. Preclinical profile of the HER2-targeting ADC SYD983/SYD985: introduction of a new duocarmycin-based linker-drug platform. Mol Cancer Ther 2014;13:2618–29.

Downloaded from http://aacrjournals.org/mct/article-pdf/15/5/958/1851970/958.pdf by guest on 24 August 2022

38. Wang H, Rangan VS, Sung MC, Passmore D, Kempe T, Wang X, et al. Pharmacokinetic characterization of BMS-936561, an anti-CD70 antibody-drug conjugate, in preclinical animal species and prediction of its pharmacokinetics in humans. Biopharm Drug Dispos 2015.
39. Lyon RP, Bovee TD, Doronina SO, Burke PJ, Hunter JH, Neff-LaFord HD, et al. Reducing hydrophobicity of homogeneous antibody-drug conjugates improves pharmacokinetics and therapeutic index. Nat Biotechnol 2015;33:733–5.
40. Strop P, Delaria K, Foletti D, Witt JM, Hasa-Moreno A, Poulsen K, et al. Site-specific conjugation improves therapeutic index of antibody drug conjugates with high drug loading. Nat Biotechnol 2015;33:694–6.
41. Guemei AA, Cottrell J, Band R, Hehman H, Prudhomme M, Pavlov MV, et al. Human plasma carboxylesterase and butyrylcholinesterase enzyme activity: correlations with SN-38 pharmacokinetics during a prolonged infusion of irinotecan. Cancer Chemother Pharmacol 2001; 47:283–90.

Downloaded from http://aacrjournals.org/mct/article-pdf/15/5/958/1851970/958.pdf by guest on 24 August 2022